Flat flexible polymer heat pipes

2013 J. Micromech. Microeng. 23 015001

(http://iopscience.iop.org/0960-1317/23/1/015001)

J. Micromech. Microeng. **23** (2013) 015001 (6pp) doi:10.1088/0960-1317/23/1/015001

Flat flexible polymer heat pipes

Christopher Oshman, Qian Li, Li-Anne Liew, Ronggui Yang, Victor M Bright and Y C Lee

Department of Mechanical Engineering, University of Colorado, Boulder, CO, USA

E-mail: victor.bright@colorado.edu

Received 22 May 2012, in final form 8 October 2012
Published 30 November 2012
Online at stacks.iop.org/JMM/23/015001

Abstract

Flat, flexible, lightweight, polymer heat pipes (FPHP) were fabricated. The overall geometry of the heat pipe was 130 mm × 70 mm × 1.31 mm. A commercially available low-cost film composed of laminated sheets of low-density polyethylene terephthalate, aluminum and polyethylene layers was used as the casing. A triple-layer sintered copper woven mesh served as a liquid wicking structure, and water was the working fluid. A coarse nylon woven mesh provided space for vapor transport and mechanical rigidity. Thermal power ranging from 5 to 30 W was supplied to the evaporator while the device was flexed at 0°, 45° and 90°. The thermal resistance of the FPHP ranged from 1.2 to 3.0 K W^{-1} depending on the operating conditions while the thermal resistance for a similar-sized solid copper reference was a constant at 4.6 K W^{-1}. With 25 W power input, the thermal resistance of the liquid–vapor core of the FPHP was 23% of a copper reference sample with identical laminated polymer material. This work shows a promising combination of technologies that has the potential to usher in a new generation of highly flexible, lightweight, low-cost, high-performance thermal management solutions.

(Some figures may appear in colour only in the online journal)

List of symbols

A	condenser bar cross-sectional area (m^2)
k	thermal conductivity (W (m K)$^{-1}$)
q_{out}	heat output (W)
ΔT	temperature difference (K)
R	thermal resistance (K W^{-1})
$T_{e,avg}$	average evaporator temperature (K)
$T_{c,avg}$	average condenser temperature (K)
Δx	distance (m)

1. Introduction

Heat pipes have been used to transfer heat from electrical components since the 1980s [1]. Typical heat pipes used for the thermal management of integrated circuits up to the present day have a metallic casing structure of copper or aluminum and exhibit relatively high physical rigidity. A heat pipe that is lightweight would be advantageous for space, aircraft and portable electronic applications where the mass of devices is critical. In addition, a flexible device would have the advantage of application in multiple possible configurations where the heat sink may be out of plane with the heat source and would allow heat removal from oscillating heat sources [2].

The concept of a flexible heat pipe initially appeared in a paper published in 1970 [2]. This work characterized a metallic heat pipe with an inner diameter of 2.54 cm and an overall length of 31.1 cm. A bellowed (corrugated) tube was used in the adiabatic region for flexibility. The wicking structure was composed of four layers of stainless steel mesh and water was used as the working fluid. Testing results showed that the temperature difference between the evaporator and condenser regions increased at 45° flex and decreased at 90° flex when compared to 0° flex.

A large portion of published works on flexible heat pipes are focused on space applications. Flexible cryogenic heat pipes were developed to transfer 20 W of power at 100 K [3]. Large-scale (1.2 × 1.8 m^2) deployable heat pipe radiators were developed by NASA for the space shuttle program [4] and were designed to transfer up to 850 W of power. A number of other publications exist describing application of flexible heat pipes in cryogenic sensor cooling [5], charge coupled device (CCD) cooling on space telescopes [6] and heat removal of space systems [7–11]. There are also several

potential applications of flexible heat pipes to aircraft flight systems [12–15].

A heat pipe with a flexible adiabatic section was developed by Kishimoto [16] for electronics thermal management. The 2.1 mm ID wickless copper tube transferred 30 W of power at a thermal resistance of 1.5 K W^{-1}. A similar system was presented by Kobayashi *et al* [17]. In 2001, McDaniels and Peterson [18] presented analytical modeling and estimated the thermal conductivity of a flat, flexible, polymer heat pipe with a grooved wicking structure to be approximately 740 W $(m\ K)^{-1}$. Their application was for flexible radiators in the space industry and the technical issues they encountered were liquid and gas diffusion through the polymer and billowing of the flexible material due to pressure differentials.

A commercial thin flexible heat pipe was introduced in 2004 by Furukawa Electric Co. [19]. Termed as 'Peraflex', this product consisted of metal foil sheets with a wicking material coated with a proprietary material to promote wettability. The 0.7 mm thick device was 15 cm long and 2 cm wide and displayed a thermal resistance of 1 K W^{-1} with 4 W power input. Bending tests showed that a maximum heat transfer of 6 W occurred with a 90° flex with 1 cm bend radius.

More recently, there have been increasing interests on the development of flexible heat pipe devices. Oshman *et al* [20] fabricated a heat pipe on a flexible liquid crystal polymer substrate using micro-machining techniques compatible with printed circuit board technologies. The device transferred up to 12 W of power with an effective thermal conductivity of up to 830 W$(m\ K)^{-1}$. Odhekar *et al* [21] presented the results of testing a copper/water heat pipe with sintered copper fiber wicking from 0° to 90° flex. They found that the flex angle had little effect on the temperature distribution and resulting copper equivalence due to the deformability of the wick structure. Most recently, Wu *et al* [22] fabricated and assessed the thermal performance of a 1.8 mm thick flat polymer heat pipe using a copper mesh as the wick structure and methanol as the working fluid. The polymer casing material was replaced by copper foil in the heater and heat sink regions to decrease the thermal resistance of the casing structure. Their device was flexed up to 45° with a power input of up to 30 W. With infrared thermal images, they estimated a thermal resistance of 0.157 K W^{-1} at a 25 W power input.

In this paper, we present the details of fabrication and thermal characterization of a thin, lightweight, flexible, low-cost heat pipe. The water-charged device was capable of transferring approximately 20 W of power through a 90° flex angle with a thermal resistance of approximately one-fourth of a geometrically equivalent copper reference sample. This result shows the promise of using the device for application where the heat source or sink may display a displacement oscillation. In addition, the flexibility allows the device to be easily reconfigured where the heater and sink are out of plane. The thin polymer casing results in a very light weight device that is more suitable for flight and space applications than a similar metallic cased device.

2. Fabrication and assembly

Figure 1 shows the overall dimensions of the assembled and tested device which is 13 cm × 7 cm × 1.31 mm while the internal liquid and vapor space is 9.5 cm × 5 cm × 0.70 mm.

The casing of the flat, flexible, lightweight, polymer heat pipes (FPHP) utilized PAVVF4W material from Impak Corp. [23], which is a multilayer polymer/aluminum material, as shown schematically in figure 2.

The PAKVF4 (also popularly named Mylar®) material is a lamination of 89 μm thick linear low-density polyethylene terephthalate (LLDPET) on the inside followed by 9 μm thick Al which serves as a hermetic barrier to liquid and gas diffusion. The two outside layers are 20 μm thick polyethylene and 12 μm of PET.

The wicking structure consisted of three layers of 200 copper meshes with 51 μm wire diameter and 76 μm spacing as shown in the scanning electron microscope image in figure 3.

The layers were aligned with identical orientation and bonded with a sintering process following the procedure presented by Li and Peterson [24] where the sintering temperature was 1030 °C and was held for 150 min in an inert Argon environment. The inset of figure 3 shows a close view of the strong bond between the layers of mesh significantly reducing the contact resistance between the layers in the wick. After sintering, the meshes were coated with an atomic layer deposited (ALD) Al_2O_3/SiO_2 bi-layer coating. The bi-layer coating was a 9 nm thick layer of Al_2O_3 and 90 nm of SiO_2. Here, Al_2O_3 was for nucleation and adhesion of SiO_2, while the SiO_2 layer promoted the stable wettability of the mesh with water. This bi-layer coating has also been found to prevent corrosion [25].

The multilayer wicking structure was thermally fused into the inner layer of LLDPET. This served not only to physically bond the wick, but also decreased the thermal resistance of the casing material by bypassing heat flow through the inner LLDPET layer. A woven nylon mesh with a wire diameter of 0.438 mm and a wire gap of 0.823 mm served as a spacer to allow vapor flow from the evaporator to the condenser. In addition to bonding the wick to the bottom casing layer, an additional layer of Mylar® was bonded to the inside of the top layer to increase the film's rigidity and mitigate the collapse of the material under high vacuum.

Prior to final assembly, all inner surfaces were cleaned with acetone and isopropyl alcohol, dried with nitrogen gas and then received a final cleaning in O_2 plasma for 45 s. The device was sealed on three edges using thermal bonding. The fourth edge was sealed with high-vacuum epoxy, including a 1 mm outer diameter copper evacuation/charging tube.

Once fully assembled, the flat polymer heat pipe was fitted to a turbo-molecular vacuum pump and evacuated to a pressure of approximately 1.5 × 10^{-6} torr. During evacuation, the device was held on a hot plate set to 40 °C to promote any outgassing from the inner surfaces. Initial pressure increased with heating, which indicated gas release from the inner LLDPET film and the nylon vapor mesh. However, a pressure which attained a level of 1.5 × 10^{-6} torr or below indicated

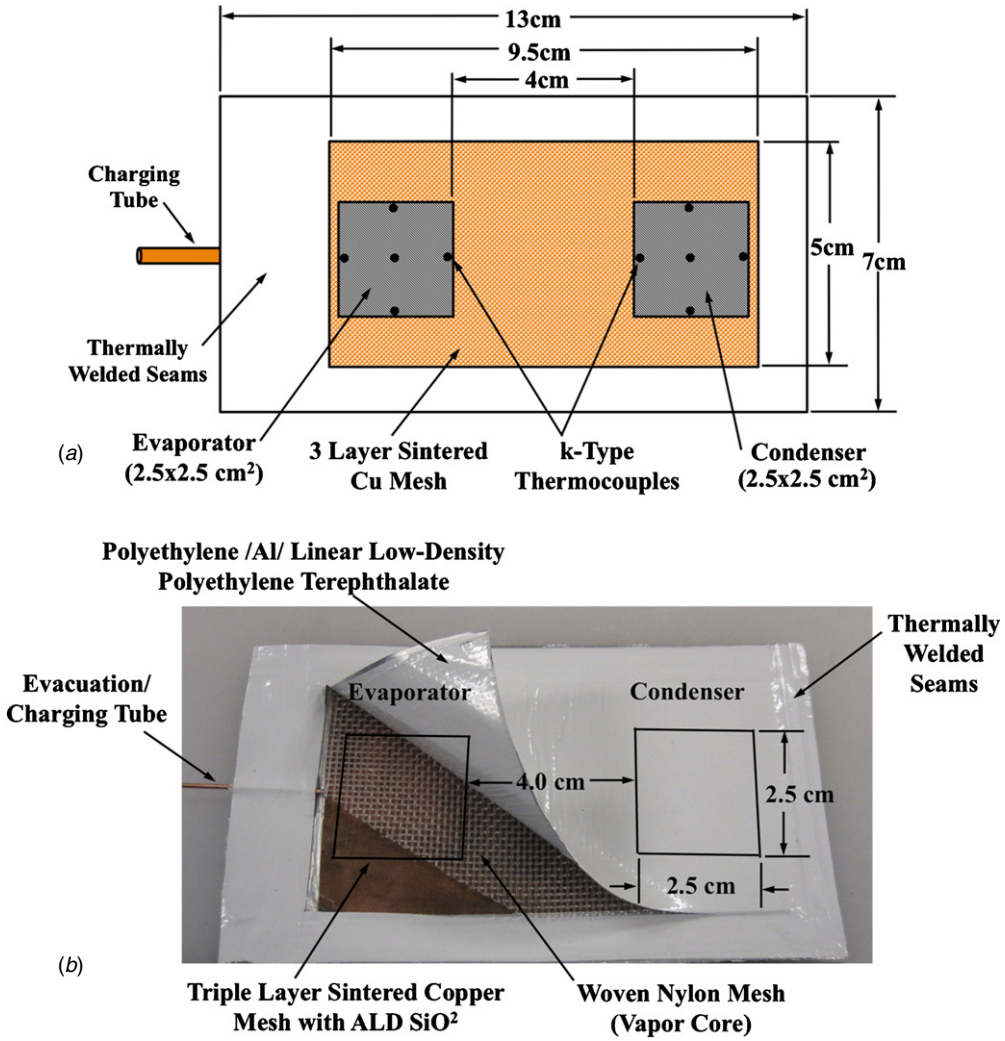

Figure 1. (*a*) Layout of the FPHP showing the location of the evaporator and condenser regions and the thermocouple placements. (*b*) Cut-away view of the assembled FPHP showing the copper mesh wicking structure, nylon vapor material and the placement of the heater and heat sink.

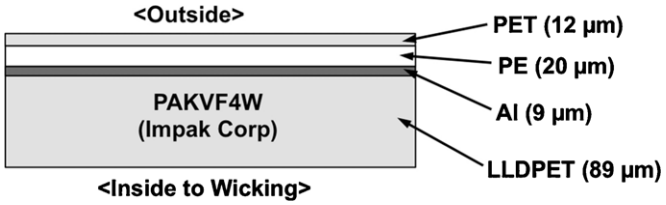

Figure 2. Cross-section of the casing material showing the laminated structure of the PAKVF4W material.

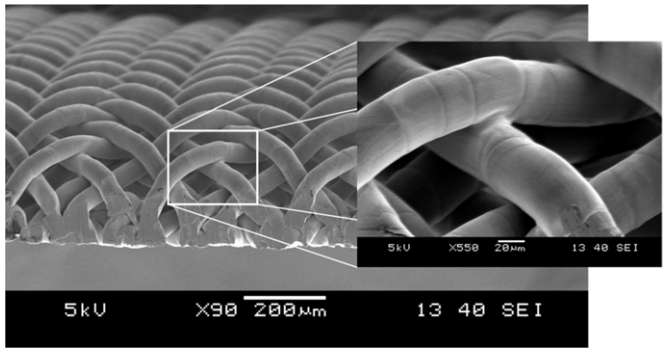

Figure 3. Scanning electron microscope image of the triple-layer sintered copper mesh that served as a liquid wicking structure for the FPHP. The inset shows a strong sintered bond formed between contacting surfaces.

a well-sealed and thoroughly out-gassed device. A quantity of 0.748 ml of distilled and de-gassed water was charged into the heat pipe. The optimum water charge was found by operating the devices with different volumes of water when the evaporator temperature was at a minimum and the condenser temperature was at a maximum. The charging tube was sealed with a cold weld using a pinch-off tool. The internal pressure after charging and sealing was depended on the internal fluid temperature and was calculated to range from 3161 Pa at room temperature (25 °C) to 21 757 Pa at the highest average operational temperature (62 °C). The pressure was always found to be below atmospheric pressure since an internal pressure greater than atmospheric would have caused the device to inflate and increase its volume, which was not observed.

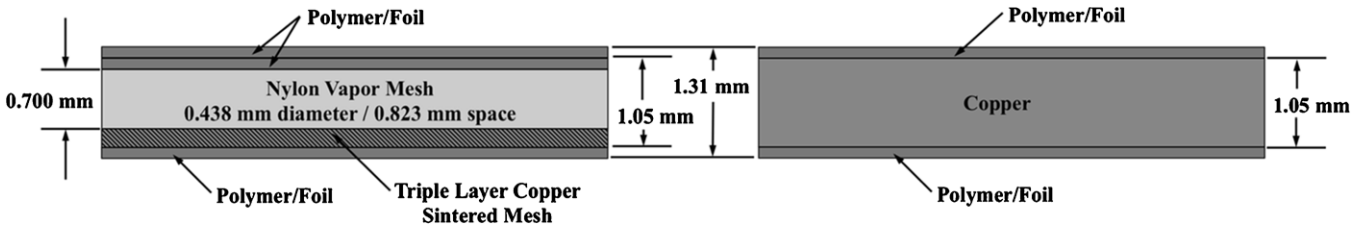

Figure 4. Cross-section showing materials and thickness for the FPHP and the copper reference sample.

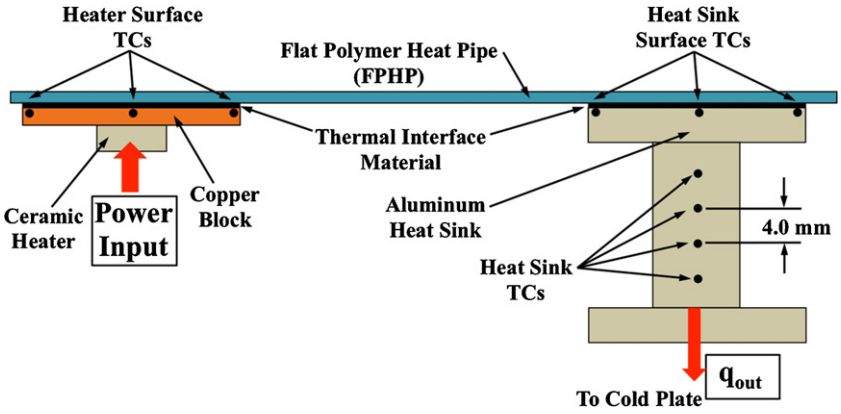

Figure 5. Cross-section of the experimental apparatus used to measure the FPHP thermal performance.

3. Thermal performance assessment

In order to assess the performance of the flexible polymer heat pipe, its thermal characteristics were compared to a reference sample of oxygen-free electrolytic solid copper (alloy 101) with identical geometric features. The total overall thickness of the FPHP was 1.31 mm. The copper reference was 1.05 mm thick and with the laminated polymer material bonded to both sides was identical in thickness to the heat pipe. Both sample cross-sections are shown in figure 4.

Heat was supplied to the 25 × 25 mm^2 evaporator region with an 8 × 8 cm^2 ceramic heater mounted to a copper block. An array of five K-type thermocouples (TCs) were embedded into the surface of the copper heater block and arranged as shown in figure 1(*a*) and in a cross-sectional view in figure 5. Thermally conductive epoxy was used to permanently seal the TCs into the block.

At a distance of 40 mm from the evaporator, heat was extracted from the 25 × 25 mm^2 condenser region with an aluminum heat sink mounted to a cold plate supplied with 10 °C chilled water. Similarly, five TCs were embedded into the contact surface of the aluminum heat sink bar to monitor the condenser temperatures also as shown in figure 1(*a*). The center bar of the heat sink was 10 × 10 mm^2 and was highly insulated, and the temperature gradient along its length was measured with a linear array of four K-type TCs fixed into the center of the aluminum bar at a distance of 4.0 mm each. Fourier's law was then used to determine the actual heat being transferred using the relation

$$q_{\text{out}} = kA\frac{\Delta T}{\Delta x}, \tag{1}$$

where k is the thermal conductivity of the aluminum heat sink, A is the cross-sectional area of the heat sink and $\Delta T/\Delta x$ is the temperature gradient along the length of the heat sink.

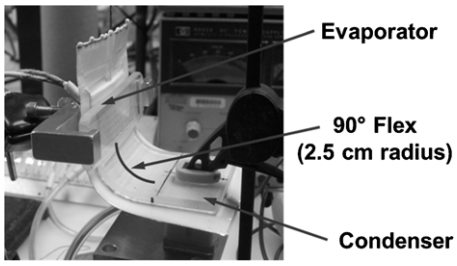

Figure 6. Apparatus used to assess the thermal performance characteristics of the FPHP at 0°, 45° and 90° flex angles.

One of the goals of this work was to create a device that exhibited good thermal performance at flex angles up to 90°. The fixture given in figure 6 shows the FPHP mounted in the experimental flexing apparatus.

The heater was clamped onto the device and contacted using a thermal interface material (TIM, Omegatherm 201). The insulated aluminum heat sink was clamped and also contacted using the same TIM. During flexing, an acrylic form was used to maintain a 25 mm flex radius as the evaporator end was raised from 0° to 45° and 90° positions.

4. Thermal performance evaluation

The thermal performance was assessed with an applied electrical power ranging from 5 to 30 W (±0.06–±0.16 W) with a dc power supply. For each power level, the FPHP was held at 0°, 45° and 90° flex angles for 10 min each to ensure steady-state operation.

The temperature difference between the heater and the heat sink was calculated as

$$\Delta T = T_{e,\text{avg}} - T_{c,\text{avg}}, \tag{2}$$

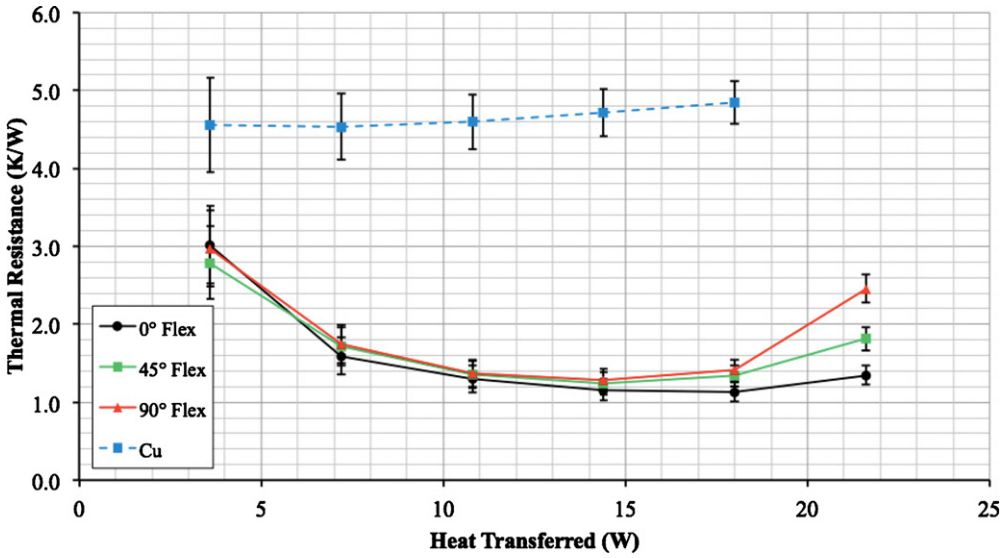

Figure 7. Plot showing the thermal resistance and heat transferred by the FPHP and copper reference sample at input powers ranging from 5 to 30 W.

where $T_{e,\mathrm{avg}}$ and $T_{c,\mathrm{avg}}$ are the average temperatures of the heater (evaporator) and the heat sink (condenser) for which the readings of multiple thermocouples at the evaporator and condenser sides were arithmetically averaged. The resulting temperature difference between the heater and the heat sink was in the range of 10–15 °C for all samples with up to 3.5 W heat transfer. As the power input was increased, the ΔT increase for copper was roughly linear and of larger magnitude than the FPHP. Testing was halted when the evaporator temperature reached 110 °C as this is a common cut-off temperature for integrated circuit protection. The effect of flex angle on the device was negligible until 18–21.5 W heat transfer and as expected the temperature difference was higher for larger angles of flex. There are two explanations for this phenomenon. The most obvious reason is that the flexure alters the geometry and increases the flow resistance of the liquid wicking structure and vapor space. Another explanation is that since the evaporator is being raised above the level of the condenser during flexure, a hydrostatic component of pressure loss is introduced into the system, decreasing the excess capillary pressure and increasing the temperature difference.

The actual heat transferred through the device and copper reference was measured and all configurations transferred approximately 72% of the applied power input until 30 W where the FPHP performance began deteriorating with 45° and 90° flex. The copper reference sample displayed consistently lower heat transfer ability due to its higher operating temperature and resulting higher convective and radiative heat losses.

The thermal resistance was then defined as

$$R = \frac{\Delta T}{q_{\mathrm{out}}} \tag{3}$$

using the experimental temperature difference and the actual heat transferred. Figure 7 shows the thermal resistance of the flexed FPHP and the copper reference sample.

It can be seen that the thermal resistance of the copper sample remained nearly constant at around 4.6 K W^{-1} for all power inputs. The copper did exhibit a slight increase in thermal resistance due to the excessive convective and radiative heat losses at higher operating temperatures. The thermal resistance of the FPHP decreased from 3.0 to 1.2 K W^{-1} at power input levels from 5 to 25 W for all flex angles. This behavior is typical of a functioning heat pipe as the temperature difference between the evaporator and condenser regions remains nearly constant (or increases slightly) while the heat transfer increases linearly with increasing power input. Beyond 18 W of heat transfer, the thermal resistance of the device increased. This increase is an indicator of the beginning of a dry-out condition in the evaporator where the viscous pressure loss of the liquid surpasses the capillary pumping pressure of the wicking structure. Also, the flex angle showed some influence on the thermal resistance where 90° flex resulted in a higher thermal resistance than 45° flex.

The FPHP is at a disadvantage to metallic heat pipes due to the high thermal resistance of the polymer-based casing material. As shown previously, the casing material was composed of four layers LLDEPT, Al, PE and PET which results in a high thermal resistance of the casing structures, from the heater to the evaporator and from the condenser to the heat sink. Also as stated earlier, the copper mesh wicking material was thermally fused into the inner layer of LLDPET. Assuming that the mesh was pressed completely through the LLDPET to the Al layer, the total calculated thermal resistance of the remaining casing is 0.475 K W^{-1}. If the polymer layer was replaced by a higher conductivity material such as copper foil [22] or a structure such as copper-filled thermal vias [20], the overall thermal resistance of the FPHP would be as low as 0.66 K W^{-1}. This is an approximately 4.6 times decrease in thermal resistance compared to solid copper. In addition to high heat transfer performance and flexibility, the mass of the FPHP was only 9.5 g compared to 46 g for the copper reference sample.

5. Conclusion

A FPHP was developed. The casing was composed of laminated sheets of LDPET, aluminum and polyethylene layers. It used a triple-layer sintered copper mesh as the liquid wicking structure and water as the working fluid. The thermal resistance was assessed from 5 to 30 W power input and from 0° to 90° flex angle. The resulting temperature difference between the evaporator and condenser regions was approximately one-fourth that of a geometrically equivalent copper reference sample at 25 W power input. The resulting thermal resistance decreased with power input to a value less than one-fourth that of a similarly configured copper reference sample. Flex angle showed little effect on the performance until the highest heat transfer levels was reached. The conclusion is that the flex angle had little noticeable effect on the heat pipe performance due to the retention of the vapor transport space by the nylon mesh and the flexibility/reliability of the liquid wicking structure.

When the calculated thermal resistance of the polymer casing is subtracted from the overall measured value and replaced with copper foil or copper-filled thermal vias, the effective thermal conductivity of the device would be approximately 4.6 times the conductivity of copper. Additionally, the mass of the FPHP was only 9.5 g, or 1/5 the mass of the copper reference. This device shows the promise of very high performance, flexible, light-weight and inexpensive thermal management solutions for the next generation of heat generation components and systems.

Acknowledgments

This work was supported by the DARPA Thermal Ground Plane Program managed by Dr Thomas W Kenny and Dr Avram Bar-Cohen (N66001-08-C-2006). The views expressed are those of the author and do not reflect the official policy or position of the Department of Defense or the US Government.

References

[1] Peterson G P 1994 *An Introduction to Heat Pipes* (New York: Wiley)
[2] Bliss F E, Clark E G and Stein B 1970 Construction and test of a flexible heat pipe *Proc. ASME Space Systems and Thermal Technologies for the 70's* pp 1–7
[3] Saaski E W and Wright J P 1975 A flexible cryogenic heat pipe *Proc. AIAA 10th Thermophysics Conf. (Denver, CO)* pp 1–5
[4] Edelstein F 1975 Deployable heat pipe radiator *NASA Final Report* NASA-CR-143863
[5] Wright J P, Brennan P J and McCreight C R 1976 Development and test of two flexible cryogenic heat pipes *Proc. AIAA 11th Thermophysics Conf. (San Diego, CA)* pp 1–8
[6] Schweickart R B and Buchko M M 1998 Flexible heat pipes for CCD cooling on the advanced camera for surveys *Proc. 5th Space Telescopes and Instruments (Kona, HI)* pp 292–300
[7] Shaubach R M and Gernert N J 1985 High performance flexible heat pipes *Proc. AIAA 20th Thermophysics Conf. (Williamsburg, VA)* pp 1–7
[8] Hwangbo H and Joost T E 1988 A flexible variable conductance heat pipe design for temperature control of spacecraft equipment *Proc. AIAA Thermophysics, Plasmadynamics, and Lasers Conf. (San Antonio, TX)* pp 1–7
[9] Gus'kov A S, Goryshov Y F and Yu A 1993 Calculation of thermophysical characteristics of an arterial flexible heat pipe *Izv. Vyssh. Uchebn. Zaved. Aviats. Tekh.* **4** 38–43
[10] Zelenov I A, Zuev V G and Poskonin U A 1996 Flexible heat pipes, construction special features and test results *Proc. ESA Int. Conf. on Spacecraft Structures, Materials, and Mechanical Testing (Noordwijk, the Netherlands)* pp 1381–4
[11] Glass D E, Stevens J C and Raman V V 1999 Flexible heat pipes for a lightweight spacecraft radiator *J. Spacecr. Rockets* **36** 711–8
[12] Gernert N J 1989 Flexible heat pipe cold plate *Final Report Naval Air Development Center, Warminster, PA* NADC 89067-60
[13] Gernert N J, Sarraf D and Steinberg M 1991 Flexible heat pipe cold plates for aircraft thermal control *Proc. SAE Aerospace Technology Conf. and Exposition (Long Beach, CA)* pp 1–72
[14] Gernert N J and Brown J 1995 Development of a flexible loop heat pipe cold plate *Proc. SAE Aerospace Atlantic Conf. (Dayton, OH)*
[15] Thomas S K and Yerkes K L 1997 Quasi-steady-state performance of a heat pipe subjected to transient acceleration loadings *J. Thermophys. Heat Transfer* **11** 306–9
[16] Kishimoto T 1994 Flexible-heat-pipe cooling for high-power devices *Int. J. Microcircuits Electron. Packag.* **17** 98–107
[17] Kobayashi T, Ogushi T, Haga S, Ozaki E and Fujii M 2003 Heat transfer performance of a flexible looped heat pipe using R134a as a working fluid: proposal for a method to predict the maximum heat transfer rate of FLHP *Heat Transfer-Asian Res.* **32** 306–18
[18] McDaniels D and Peterson G P 2001 Investigation of polymer based micro heat pipes for a flexible spacecraft radiator *Proc. ASME Int. Mechanical Engineering Congress and Exposition (New York, NY)* pp 423–33
[19] 2004 Ultra-thin sheet-shaped heatpipe 'Pera-flex' *Furukawa Rev.* **25** 64–6 (www.furukawa.co.jp/review/)
[20] Oshman C, Shi B, Li C, Yang R G, Lee Y C, Peterson G P and Bright V M 2011 The development of polymer-based flat heat pipes *J. Microelectromech. Syst.* **20** 410–417
[21] Odhekar D D and Harris D K 2011 Bendable heat pipes using sintered metal felt wicks *Front. Heat Pipes* **2** 1–8
[22] Wu G W, Shih W P and Chen S L 2011 Lamination and characterization of a PET flexible micro heat pipe *Proc. 10th Int. Heat Pipe Symp. (Taipei, Taiwan)* pp 1–6
[23] Impak Corporation www.impakcorp.com
[24] Li C and Peterson G P 2006 The effective thermal conductivity of wire screen *Int. J. Heat Mass Transfer* **49** 4095–105
[25] Phan H T, Caney N, Marty P, Colasson S and Gavillet J 2009 Surface wettability control by nanocoating: the effects on pool boiling heat transfer and nucleation mechanism *Int. J. Heat Mass Transfer* **52** 5459–71